# Digital laser micro- and nanoprinting

Qingfeng Li, David Grojo, Anne-Patricia Alloncle, Boris Chichkov, Philippe Delaporte

Review article

Qingfeng Li, David Grojo, Anne-Patricia Alloncle, Boris Chichkov and Philippe Delaporte*

# Digital laser micro- and nanoprinting

https://doi.org/10.1515/nanoph-2018-0103
Received July 23, 2018; revised September 27, 2018; accepted September 28, 2018

**Abstract:** Laser direct writing is a well-established ablation technology for high-resolution patterning of surfaces, and since the development of additive manufacturing, laser processes have also appeared very attractive for the digital fabrication of three-dimensional (3D) objects at the macro-scale, from few millimeters to meters. On the other hand, laser-induced forward transfer (LIFT) has demonstrated its ability to print a wide range of materials and to build functional micro-devices. For many years, the minimum size of laser-printed pixels was few tens of micrometers and is usually organized in two dimensions. Recently, new approaches have been investigated, and the potential of LIFT technology for printing 2D and 3D sub-micrometer structures has become real. After a brief description of the LIFT process, this review presents the pros and cons of the different digital laser printing technologies in the aim of the additive nanomanufacturing application. The transfer of micro- and nano-dots in the liquid phase from a solid donor film appears to be the most promising approach to reach the goal of 3D nanofabrication, and the latest achievements obtained with this method are presented and discussed.

**Keywords:** micro- and nanofabrication; high-resolution patterning; laser-induced forward transfer.

## 1 Introduction

Nature continuously produces and benefits from the unique properties exhibited by nanostructured materials. In recent years, there is an increasing number of studies focused on the development of strategies to mimic these natural properties [1–3] by producing nanomaterials and nanostructures to access new attractive properties and functionalities in various domains (optical [4, 5], thermal [6], mechanical [7, 8], etc.). This has led to the emergence of new fields of research like nanophotonics [9, 10], nanochemistry [11, 12] and nanomedicine [13], among others. Nanostructures, like arrays of pillars or dots, have been extensively used in the field of energy to enhance the absorption of light, thanks to the localized surface plasmon resonance effect [14]. For instance, gold nanopillars have been used to enhance the photocatalytic activity of iron oxide in the water splitting approach to produce hydrogen fuel from solar energy [15]. Figure 1 provides a set of nanostructures that have been designed and realized for nanophotonics applications. For instance, Yagi-Uda antenna, aiming at highly directional radiation of greater power, can be formed by nanoparticles of different diameters precisely aligned with accurate separation distances (Figure 1A) [16, 19]. Arrays of nanoantennas based on V-shaped plasmonic nanoparticles carefully organized on surfaces, in a fashion similar to that presented in Figure 1B, provide a powerful way to control the reflection and refraction of light, including negative refraction. This allows the development of applications such as spatial phase modulation, beam shaping, and plasmonic lenses [20]. Figure 1C and D presents other two-dimensional (2D) designs of antennas based on the association of different shapes and different materials. Complex 3D nanostructures are also of interest for nanophotonics applications, and Figure 1E and F presents arrays of left- and right-handed metallic nanospiral that have been realized to study and exploit chiroptical material responses [18]. These few examples illustrate the challenges that have to be faced to develop an ultra-high-resolution deposition technique to print such different materials with various shapes and sizes and a high positioning accuracy. This paper will discuss how the laser printing technology can contribute to the development of these fabrication technologies.

Accurately mimicking natural nanostructures is a difficult challenge requiring interdisciplinary approaches to address the problems of morphology, the physical and chemical properties of the materials, and biological

*Corresponding author: Philippe Delaporte, Aix-Marseille University, CNRS, LP3 Laboratory, 13009 Marseille, France, e-mail: philippe.delaporte@univ-amu.fr.
https://orcid.org/0000-0002-3721-741X
Qingfeng Li, David Grojo and Anne-Patricia Alloncle: Aix-Marseille University, CNRS, LP3 Laboratory, 13009 Marseille, France
Boris Chichkov: Leibniz Universität Hannover, Institut für Quantenoptik, Welfengarten 1, 30167 Hannover, Germany

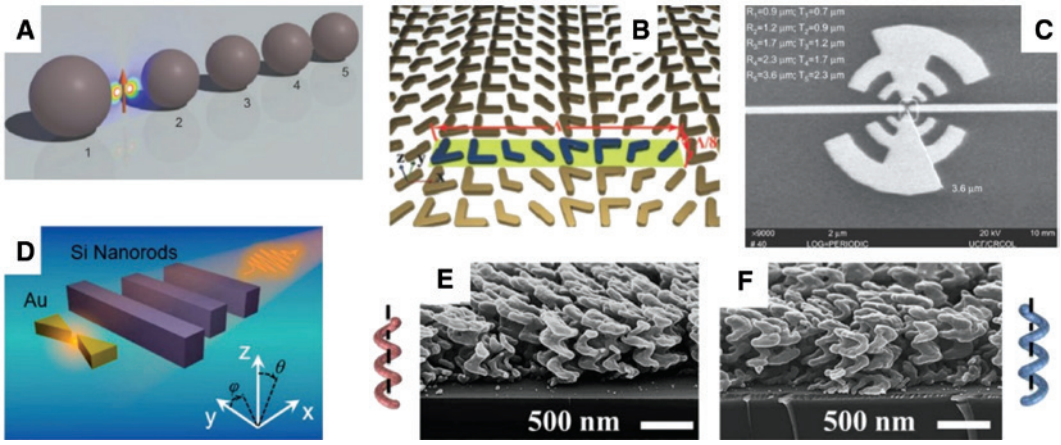


**Figure 1:** Examples of 2D and 3D nanostructures designed for nanophotonics applications.
Designs of nanoantennas based on nanoparticles (A) and V-shaped (B) structures. Optical antenna coupled to a microbolometer (C). Design of a hybrid Au-Si Yagi-Uda nanoantenna (D). Left- (E) and right- (F) handed arrays of silver nanospirals. (A–C) Reprinted with permission from Ref. [16]. (D) Reprinted with permission from Ref. [17]. (E) and (F) Reprinted with permission from Ref. [18].

interactions with the environment. The first step to carry out these studies is to have available, or to develop, technologies of micro- and nanofabrication, either subtractive or additive.

Among the nanomanufacturing technologies photolithography is probably the most widely used to pattern surfaces at the nanoscale (down to 10 nm), but it is a costly, time-consuming, and low-throughput process. In the same category of mask-based technology, nanoimprint lithography [21, 22], microcontact printing [23], and transfer printing [24, 25] appear to be high-resolution and low-cost techniques to realize nanostructures from predefined molds or stamps. Lasers are also powerful tools to develop non-contact surface patterning technologies [26]. Among them, one can cite microsphere-assisted methods in which a single laser shot irradiates a large-area sample through a monolayer of microspheres to induce a local ablation of the substrate underneath each sphere, thanks to the near-field exaltation of the laser field. Then, this parallel nano-ablation process allows the formation of arrays of nano-holes [27] and of nano-dots [28], with sizes as small as 100 nm. For a similar prospect, direct laser interference patterning [29] is also a very efficient tool for structuring surfaces at the sub-micrometer scale with a predefined pattern and with high throughput [30]. In addition to its high process speed, the periodicity of the nanostructures can be optically tuned by changing the interference design and their aspect ratio is controlled by the number of laser shots. Without structuring the intensity distribution, laser irradiation under appropriate conditions can also induce the spontaneous formation of self-organized structures, as spikes or ripples, which are the two most studied shapes obtained, thanks to this approach. Both types of structures strongly modify the surface properties [31]. Spikes [32, 33], with typical diameter of 1 µm, enhance visible-light absorption of silicon and potentially the efficiency of solar cells [34] and the sensitivity of photodetectors [35]. They also provide a super hydrophobicity character [1, 31] to the surfaces to address applications such anti-icing or anti-bacteriological properties. Ripples are composed of parallel engraved lines at the substrate surface whose orientation is controlled with laser polarization and the period by the laser wavelength. Such structures have been used, for instance, to control the motion of fluids onto surfaces [36] and as optical diffraction grating in the visible domain of the spectrum [37]. Laser dewetting is another very easy to implement technique to produce nano-patterned surfaces. It consists of the irradiation by a nanosecond laser pulse, with a uniform beam energy profile, of a thin metal film deposited on a substrate. The laser irradiation induces a very fast heating of the film and, depending on the surface energies of the melted film and the substrate, its dewetting forms a network of metal nanodroplets [38].

Direct femtosecond laser writing has also been used to locally transform a silver oxide film in silver nanoparticles with diameter of few tens of nanometers [39]. These laser-fabricated plasmonic structures have demonstrated their potential in the field of nanochemistry by improving the efficiency of hydrogen generation when formed on the photoelectrodes of a water splitting system [40] and to fabricate active substrates for surface-enhanced Raman scattering measurement [41]. Backside irradiation, with a tightly focused ultrashort pulse, of a thin film coated on a transparent substrate leads to the formation of a nanobump [42–45] or an array of nanobumps when multispots are used [46]. This method has been used to form

plasmonic structures, allowing 3D control of light propagation [44, 46].

Digital manufacturing is also extremely attractive for its ability to be fully computer controlled and easy to integrate in any fabrication process. Inkjet printing [47] has been extensively developed, especially for electronic applications [48], and it is a very powerful technique for high-speed printing of micrometer-sized liquid droplets. However, it has some limitations in (i) the type and viscosity of liquids that can be transferred, (ii) the minimum size of the printed structures hardly smaller than few tens of micrometers and (iii) the aspect ratio that can be achieved for the printed structures. Recently, an electrohydrodynamic printing technology, named NanoDrip printing, has been introduced [49]. It allows printing 3D structures with size down to 50 nm and a very good resolution, as well as free-standing nanowires [50]. Direct laser writing also offers the possibility to develop some digital printing technologies. Multiphoton polymerization is a very promising 3D micro/nanomanufacturing technique [51]. It relies on the simultaneous absorption of two or more infrared photons to locally initiate the polymerization mechanisms and has been used to fabricate objects with sub-100 nm resolution [52]. This technology offers great opportunities for the fabrication of micro/nanophotonics devices [53] and biomedical scaffolds for tissue engineering [54, 55]. Laser writing has also been combined with chemistry to trigger the photoreduction process for the realization of 3D metallic structures [56].

Laser printing is a generic term to describe processes in which a laser pulse irradiation induces the transfer of a small amount of matter from a donor film to a receiver substrate at a very precise location. The most popular approach based on this concept is the laser-induced forward transfer (LIFT) technique, described in Figure 3, and it has been first demonstrated by Bohandy et al. [58]. Some LIFT-based techniques have also been developed for specific applications, like Decal transfer for the printing of high-viscosity pastes [59]; blister actuated LIFT when using an intermediate polyimide film [60]; film-free LIFT, where the thin donor film is replaced by a liquid reservoir [61]; or the double-pulse LIFT [62]. These various approaches have been successfully implemented to print 2D structures of a large set of materials, organic and inorganic, in solid or liquid phase, and to fabricate functional devices [63–67]. LIFT has also demonstrated its ability to operate at high printing velocity [68, 69]. We should also mention the great potential of LIFT for printing biomaterials [70–72]. Indeed, the ability of this technique to precisely deposit droplets of liquid with different viscosities makes it particularly suitable for tissue engineering applications [73, 74].

However, apart from the results obtained by Pique's group [75, 76] using high-viscosity silver nanopastes, there have been only a few demonstrations of 3D printing with sub-15 μm resolution until recently. Indeed, the last few years, there has been an increasing number of studies presenting the fabrication of micrometer 3D structures or 2D arrays of inorganic nanodots by means of laser printing, which reveals the potential of LIFT to add to the panel of the attractive nanofabrication techniques [77]. Figure 2 shows a typical experimental arrangement for

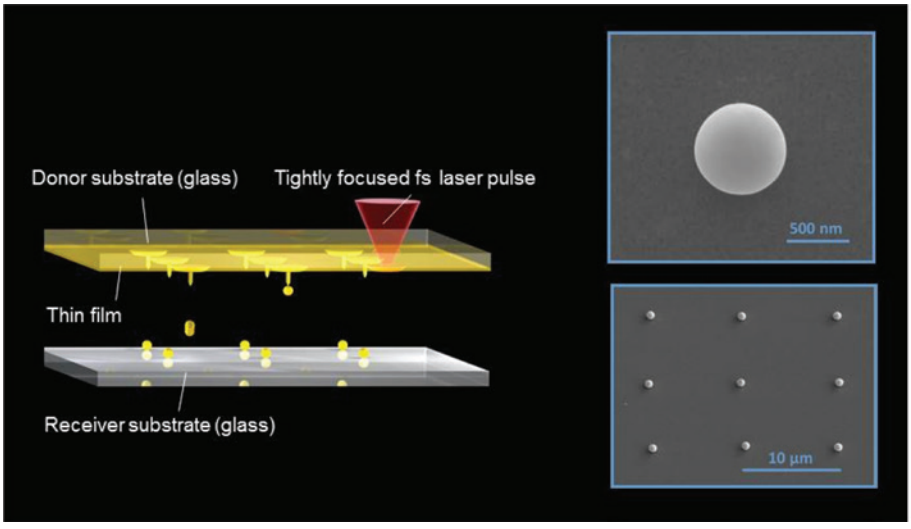


**Figure 2:** Typical experimental setup for laser printing of nanoparticles is shown on the left side. SEM images of a single printed gold nanoparticle and nanoparticle array are shown at the right side.

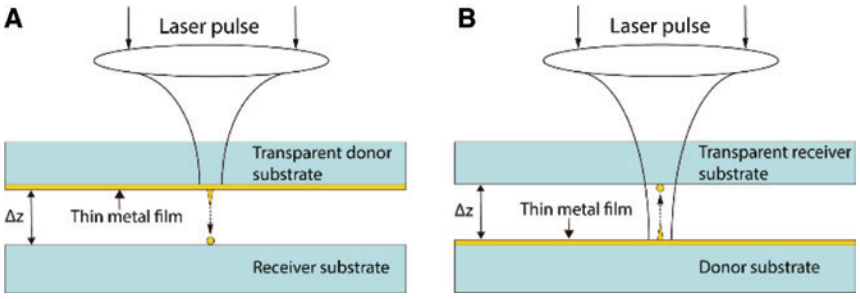


**Figure 3:** Schematic view of arrangements for the so-called (A) laser-induced forward transfer (LIFT) and (B) laser-induced backward transfer (LIBT).
In LIFT mode the laser irradiates the metal film through the transparent donor substrate while in LIBT mode the laser irradiates the thin film through the receiver substrate. Adapted and with permission from Ref. [57].

laser printing of nanoparticles. The figure is accompanied by scanning electron microscopy (SEM) images of a single printed gold nanoparticle and a nanoparticle array evidencing the level of repeatability of the printing process. After a brief description of the LIFT process, this review presents the state of the art results in micro- and nanofabrication and discusses the potential of LIFT as a digital additive nanomanufacturing process.

# 2 Physics of laser-induced transfer

## 2.1 Principle of operation

As shown in Figure 3A, the LIFT process consists of the irradiation, using a pulsed laser, of a thin film of an absorbing material (the donor) previously deposited onto a transparent substrate. This donor is irradiated through the substrate, and the laser interaction at the interface induces the ejection of a small part of the irradiated material and its deposition onto a target substrate (the receiver) set in close proximity. The donor can be a solid film and the pixel is then transferred in solid phase, or a liquid film and a droplet are then deposited onto the receiver substrate. The laser-induced backward transfer (LIBT) configuration is represented in Figure 3B. The top surface of the donor film is irradiated through a transparent receiver substrate, and materials are transferred by ejection from the film by physical mechanisms that are loosely analogous to those in the LIFT configuration. If the thin film is transparent to the laser irradiation, then the laser energy is absorbed by the donor substrate at the interface, as for the LIFT configuration. If the laser energy is absorbed by the film, then, under some conditions discussed later, its fast deformation can lead to the ejection of a droplet.

The physics and the potential of these laser printing processes have been previously discussed in numerous papers [78–82]. Laser printing from both solid and liquid films exhibits numerous advantages, which are not discussed here, but also some drawbacks, which are more or less pronounced depending on the donor material properties. Here, for clarity, we can draw some very general features for each configuration.

### 2.1.1 LIFT in the solid phase

The physics of LIFT in the solid phase relies on the fast heating of the donor film, leading to a strong increase in pressure in the confined volume of the irradiation zone, at the interface between the donor film and the transparent substrate. This effect induces mechanical forces that break the film and propel it toward the receiver. This ejection dynamics has been extensively studied by means of time-resolved shadowgraphy technique [83] that has helped in identifying two main drawbacks of the approach. First, a shock wave is generated at the surface of the film, which propagates in front of the flyer, reflects onto the receiver, and can destroy the flyer when crossing it [84]. Second, a significant amount of debris is induced by the laser-matter interaction process, and they are also deposited onto the receiver. Different strategies have been developed to prevent the generation of debris. We can mention the use of an intermediate layer between the substrate and the donor film to reduce the laser-induced heating of the film [85, 86] or the use of smart beam shaping [87]. They appear quite efficient for the printing of organic materials [88–90], but very little improvement is obtained in case of inorganic compounds.

### 2.1.2 LIFT in the liquid phase

The mechanisms of LIFT in the liquid phase are quite different from those in the solid phase. The laser energy

absorbed by the liquid film induces the formation of a cavitation bubble, which first expands and pushes the liquid surrounding it. With the bubble expansion being mainly oriented perpendicularly to the substrate, the fluid motion around it leads to a high pressure point at the top of the bubble and to the formation of a liquid jet, which propagates toward the receiver and forms a droplet on it [79]. These mechanisms, theoretically suggested in 2004 by Pearson et al. [91] for a free surface configuration, have been experimentally investigated by a few groups by means of time-resolved imaging, or shadowgraphy, of the bubble formation, jet expansion, and droplet deposition [92–94]. This approach allows printing well-resolved droplets down to 15-µm diameter with a very good reproducibility and resolution. Moreover, the droplet characteristics are not modified when the distance between the donor and the receiver varies from few tens of micrometers up to 2 mm, and most importantly, no debris are generated onto the receiver substrate. However, the transfer in liquid phase has also some drawbacks. First, it is quite complex to maintain a liquid donor film with uniform properties (thickness, viscosity, and density) during the process due to the evaporation mechanism. Then, a sintering or annealing step of the printed materials is needed when metal nanoparticle inks are transferred to stabilize them and to get their final properties (conductivity). Lastly, the printing of sub-micrometer droplets requires the reduction of both the laser spot size and the liquid film thickness. However, there is a limitation on the minimum thickness, around a few micrometers, of the uniform liquid films that can be prepared due to the dewetting process. The LIFT in the liquid phase approach is especially relevant for printing biomaterial [95–99] and nanoparticle metal inks [100–103]. It is worth mentioning the blister-actuated LIFT technique [60, 104], which uses a polyimide film coated between the transparent substrate and the donor film to absorb the laser energy. This leads to the break-free deformation of the polyimide film, which induces the fluid motion and the jet formation. This technique allows printing sensitive materials and getting rid of any risk of contamination from the intermediate layer debris.

To complement this description, Table 1 summarizes the pros and cons of the two laser printing processes, from solid or liquid film as donor. These overall features are more or less pronounced depending on the donor film properties.

## 2.2 Printing solid in the liquid phase

Since the last few years, some groups [62, 105–109] have investigated a new approach to combine the advantages of the two techniques and to address the challenge of digital micro- and nanoprinting. It consists of irradiation by an ultrashort laser pulse of a thin metal donor film to melt it and to create a liquid metal jet and finally print a micro- or nanodot on the receiver substrate. It has been observed that the diameter of the printed pixel decreases with the reduction in the donor film thickness [106, 107]. Depending on the laser pulse duration and the donor film thickness, different physical mechanisms are suggested to explain the ejection process. As the first step is the melting of the whole film thickness in the irradiated area, one must pay great attention to the relation between the pulse duration and the thickness of the film, which is affected and defined by the thermally affected length $l_{th}$:

$$l_{th} = 2\sqrt{D\tau},$$

where $D$ is the thermal diffusion coefficient of the donor material and $\tau$ is the laser pulse duration. This relation should not be considered for sub-picosecond pulse duration as the electron-photon relaxation time is of

**Table 1:** Pros and cons of the LIFT processes from solid and liquid donor film.

| Donor film | Cons | Pros |
|---|---|---|
| Solid | – Generation of debris<br>– Shock wave interaction with pixel<br>– Lack of adhesion<br>– Low resolution of the pixel edges<br>– Limited minimum lateral sizes | – Donor film<br>  – Stable<br>  – Easy to handle<br>  – Very thin film<br>– No post-process<br>– Single-step printing of large area |
| Liquid | – Post-process required<br>– Donor properties vary over time (solvent evaporation)<br>– Ultrathin film not achievable | – Clean printing without debris<br>– Process velocity<br>– High resolution<br>– Less dependence to donor-receiver gap<br>– 3D printing (pastes) |

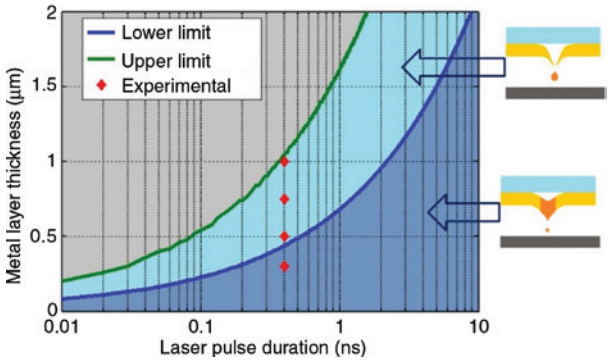


**Figure 4:** Calculated ranges of metal donor film thicknesses allowing the transfer of a single copper microdroplet for pulse durations varying from 10 ps to 10 ns.
The green (resp. blue) curve represents the maximum (resp. minimum) film thickness for a given pulse duration to induce the transfer of a single droplet under appropriate laser fluence condition. Reprinted with permission from Ref. [108]. The red diamonds correspond the experimental conditions used in Ref. [108].

picosecond time scale in metals. So, for a given pulse duration, there is only a range of film thickness that can be used to achieve its melting and the targeted debris-free printing of micro or nanodots. The laser energy must also be tuned to melt the whole film thickness without vaporizing a too large volume of donor material at the interface between the donor film and the transparent substrate. As shown by Zenou et al. [108], shorter is the laser pulse duration and smaller is the range of film thickness that can be used. Figure 4 shows the calculated ranges of the metal donor film thicknesses that allow the transfer of a single microdroplet for pulse durations from 10 ps to 10 ns. Also, we can observe in Figure 7A that the laser fluence required to fully melt a 620 nm copper film with a 50 ps laser also induces the ejection of large amount of droplets. These authors suggested a new mechanism called thermally induced nozzle to achieve a stable and highly directional jetting of metal droplets over a rather large range of donor-receiver gap (>400 µm) [110]. The main idea of this approach is to irradiate the film with a laser energy, allowing the melting of almost all the donor thickness while the fast expansion of the heated metal breaks the non-melted surface of the film. These conditions form a nozzle from which a liquid droplet is ejected. Figure 5 shows a scheme to illustrate this approach and a SEM image of the donor film after the laser irradiation and the transfer process where the thermally induced nozzle is clearly visible.

Pohl et al. [109] also printed micro-droplets by means of picosecond laser irradiation of metal donor films with thicknesses of few hundred of nanometers. They suggested different ejection mechanisms depending on the laser fluence that is applied. At low fluence, a cap ejection is observed, driven by the relaxation of thermal stresses induced by laser-induced heating. When the laser fluence increases, the thermal processes that prevail lead to liquid jet formation. Ultimately, for the highest tested fluences, they observed the vaporization of the film and the uncontrolled generation of large amounts of droplets. Both cap ejection and jet formation mechanisms are attractive for printing metal structures, but it appears difficult to avoid the deposition of unwanted satellites around them.

In order to fully benefit from all the advantages of LIFT from a liquid film, Li et al. recently proposed a new method, the double pulse LIFT, which relies on the use of two lasers [62]. A first quasi-continuous wave (QCW) laser, operating in long-pulse-duration mode, irradiates the solid donor film through the transparent substrate in order to reach the melting temperature and, thus, to locally form a liquid film. Then, a second appropriately synchronized laser pulse of short duration irradiates the central part of this area, and that induces the formation of a liquid jet and the printing of a droplet on the receiver substrate. When cooling, this metal droplet solidifies on the substrate. Figure 6 presents a scheme of the experimental setup. The dual-laser approach allows independently controlling the phase change of the donor film with the QCW laser irradiation and the transfer process in the liquid phase with an ultrashort pulse laser.

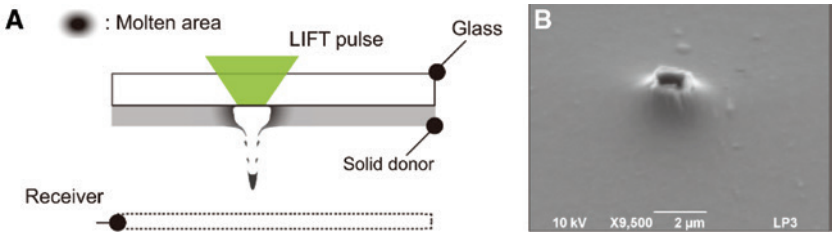


**Figure 5:** Schematic illustration of the thermally induced nozzle approach (A) and SEM image of a copper donor film after an ultrashort pulse irradiation showing the formation of a thermally induced nozzle (B).
The laser fluence is tuned to melt almost the full film thickness, and the expansion of the heated metal forms a nozzle from which is ejected a droplet.

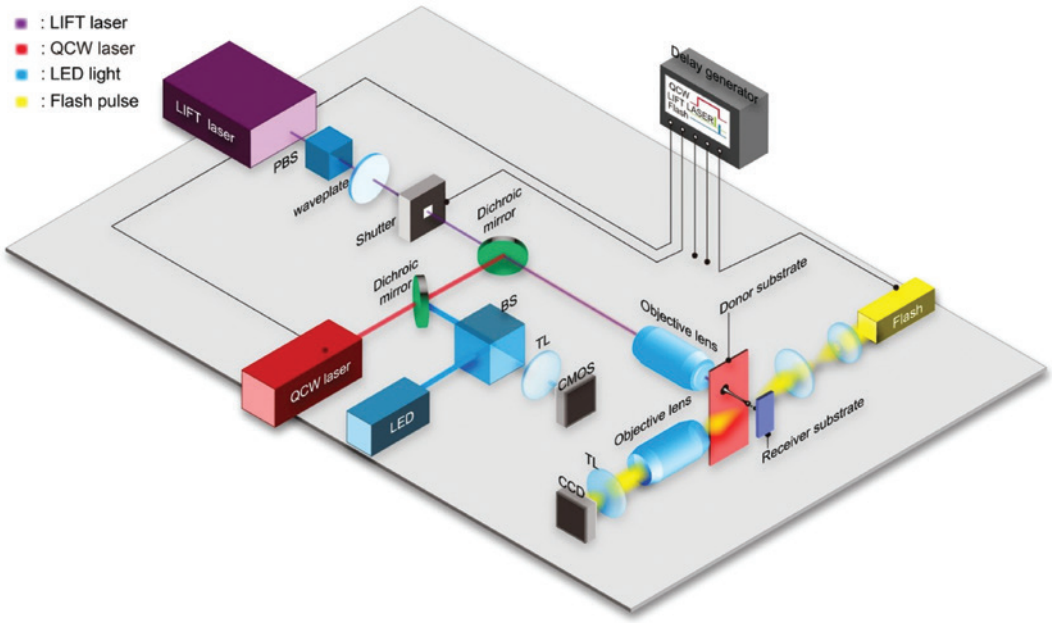


**Figure 6:** Experimental setup of the double-pulse LIFT.
The QCW laser provides long pulse irradiation to melt the film. The LIFT laser (fs or ps) induces the ejection process in the liquid phase. The flash lamp and the CCD camera are used to acquire the time-resolved shadowgraphy images.

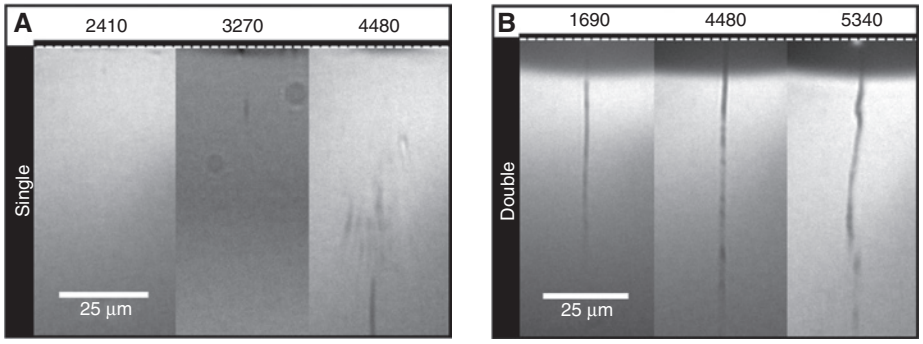


**Figure 7:** Time-resolved shadowgraphy images of ejection dynamics after the irradiation of a 620-nm-thick copper film with a single short laser pulse (A) or by two laser pulses (QCW + ps) (B). The fluence of the short pulse laser (mJ/cm$^2$) is written above each images, and all images have been acquired 280 ns after the ultrashort pulse.
One can observe that in single pulse mode the energy required to form a liquid jet also induces the ejection of unwanted debris, while in double pulse mode stable metal jets are formed over a large range of fluence. Reprinted with permission from Ref. [62].

As shown in Figure 7, this approach allows the generation of long and stable liquid metal jets over a large range of film thicknesses and laser fluences. Figure 7A shows shadowgraphy images of the ejection dynamics for different laser fluences when a single picosecond laser pulse is used to both melt and transfer the metal, while Figure 7B shows the results obtained in similar experiments when using a QCW laser irradiation prior to the picosecond laser one. For a such 620-nm-thick copper film processed in these experiments, it is impossible to form a stable liquid jet without inducing the ejection of satellites if the metal film is not previously melted by the QCW laser irradiation.

Figure 8 summarizes the increase in the process windows in terms of laser fluence and donor film thickness when using dual-laser printing compared to single-laser printing. For the latter configuration, one can observe that the process window to form a stable liquid metal jet with a picosecond laser irradiation is optimum for a specific film thickness, while stable jets are achievable for a large range of film thicknesses in the double-pulse LIFT mode of operation.

In the LIFT of the liquid process, whatever the origin of the mechanisms inducing the fluid motion, the deformation of an intermediate polymer layer in the blister

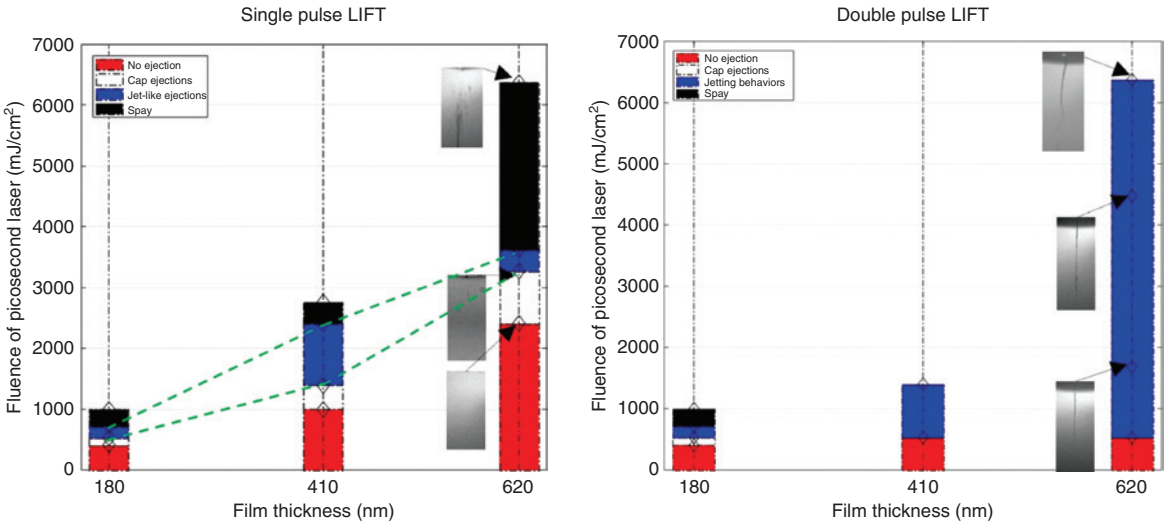


**Figure 8:** Regimes of ejection as a function of the ultrashort pulse laser fluence for the single-pulse LIFT and the double-pulse LIFT for three different thicknesses of the donor copper film.
In single pulse mode, the formation of stable jets occurs only for a narrow range of film thickness, while in double pulse mode the process window is strongly increased.

mode [111], cavitation bubble expending in the film [79], or relaxation of the laser-induced stresses inside the molten film in ultrashort pulse regime [112, 113], the formation of the liquid jet relies on a competition between the kinetic energy of the fluid moving away from the film and the surface energy of the liquid, which tends to keep the film uniform. This balance is characterized by the dimensionless Weber number ($W_e$), which is the ratio of the kinetic energy to the surface energy. Figure 9 presents some shadowgraphy images of liquid ejection after a double-pulse irradiation of a 1-μm-thick copper film. The first laser pulse locally melts the copper film and the following fs laser irradiation provides the kinetic energy to the liquid. All these images have been taken with a fixed delay of 500 ns after the fs pulse and with a temporal resolution of 20 ns. A detailed description of the experimental setup can be found elsewhere [62]. The different images correspond to different energies of the fs laser, and then to different kinetic energies. For the lowest energy, 0.15 μJ (7.3 J/cm²), the film deforms, but there is no ejection because the kinetic energy does not overcome the surface energy ($W_e < 1$). At 0.19 μJ (9.4 J/cm²), the Weber number is slightly higher than 1, so the jet forms but it immediately breaks because of surface energy and only a single droplet is ejected. A further increase in the laser energy leads to the generation of jets with increasing velocity, until instabilities appear (2.21 μJ–110 J/cm²). Printing a single droplet is the most appropriate configuration for micro-nanofabrication applications.

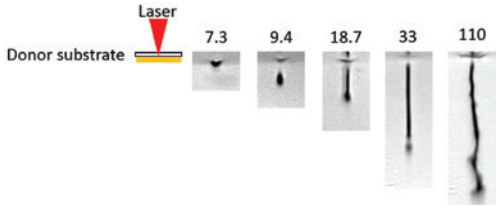


**Figure 9:** Time-resolved shadowgraphy images of the ejection of melted copper in double-pulse LIFT configuration.
The donor is a 1-μm-thick copper film and the images have been taken with a fixed delay of 500 ns after the irradiation by the fs laser pulse with a beam diameter (1/e) of 1.6 μm. Each image corresponds to a different fluence of the fs laser pulse mentioned in J/cm² above the image.

Femtosecond laser pulses have also been used to print nanodroplets from metallic films thinner than 100 nm [105, 106, 114, 115]. The laser irradiation, with a Gaussian beam profile, induces both a Gaussian distributed pressure force and the melting of the full thickness of the film in the irradiated area. Then, due to surface tension, the melted film detaches from the substrate with the shape of a dome shell. Within this layer, the normal component of the capillary forces decelerates the normal velocity of the shell, while the parallel component leads to the motion of the liquid metal toward the center of the dome. The jet starts to form when the reverse motion of the shell begins [116, 117]. Molecular dynamics simulations have helped in the understanding of the initial stage of the laser energy diffusion in the thin film [118], as well as the formation of the liquid jet and the conditions for droplet detachment from the film [119]. In particular, studies have highlighted the importance played by the beam and film sizes in the formation and expansion of the metal liquid jet. The film

thickness needs to be smaller than the thermal diffusion length to ensure complete melting of the film. Obviously, the laser fluence must be adjusted to provide enough energy for this film melting but also to keep a moderate velocity of the film motion to favor the capillary effects and the jet formation. The use of a low rigidity or deformable donor substrate helps in this way by reducing the ejection velocity for a given laser fluence. This approach has also been used to pattern a gold-coated surface with an array of frozen nanojets, thanks to its irradiation with interfering femtosecond laser beams [42].

## 3 3D laser micro-fabrication

The understanding of the laser printing process of metal droplets in the liquid phase from a solid film opens a way for the development of a new digital additive manufacturing technology at the micro-scale. Few groups have started to investigate the potential of this approach and they have obtained some very promising results. Zenou et al. explored the fabrication of 3D metal structures with the thermally induced nozzle technique [110]. They used sub-nanosecond laser pulses and micrometer-scale-thick donor metal layers to digitally print, under ambient atmospheric conditions, arbitrary micrometer-scale objects. For instance, Figure 10 shows SEM images of the LIFT-printed copper word "small" on a glass slide. The width of the printed letters was 50 μm and the height of the letters was gradually increased [120]. The printed structure consists of overlapped molten copper metal droplets, as shown in Figure 10C. They also printed copper pillars with uniform diameters as small as 8 μm and longer than 200 μm, and they successfully achieved the fabrication of tilted pillars with a maximum angle of 30° to address the challenges of printing unsupported curved structures [108]. One of the main advantages of the thermally induced nozzle approach is its ability to print with a large distance

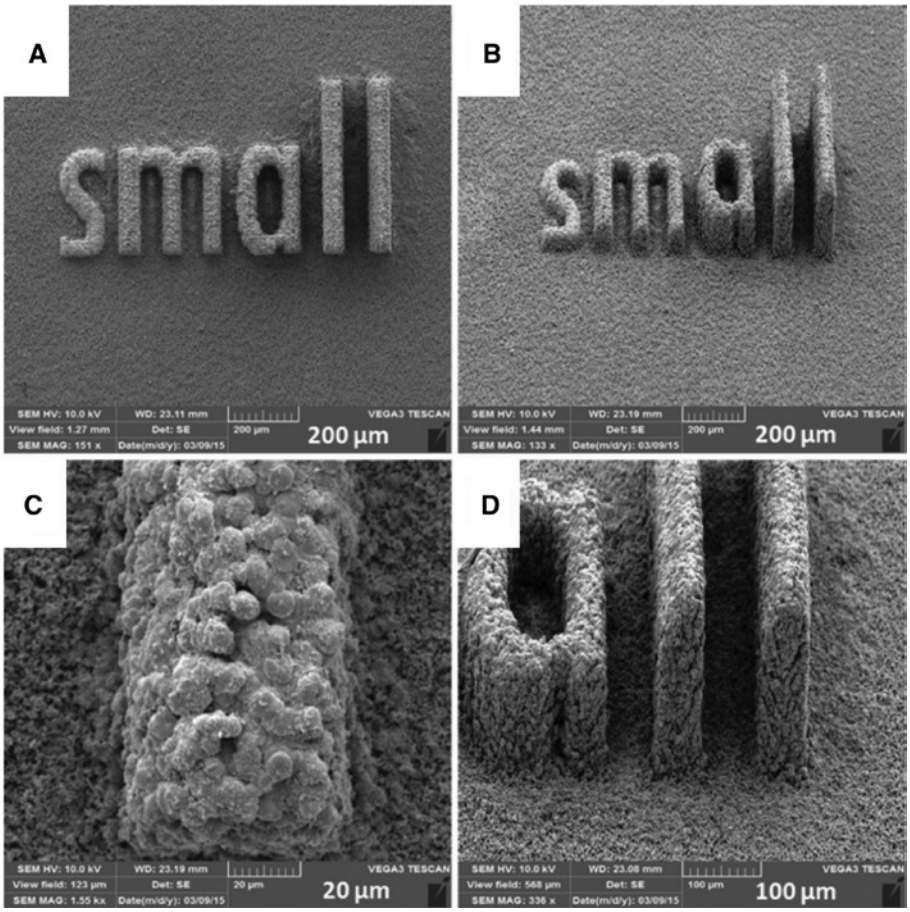


**Figure 10:** SEM images of the LIFT-printed copper word "Small" on a glass substrate (top view A, tilted view B). The width of the printed letters is 50 μm and the highs of the letters are gradually increased from 40 μm to 190 μm. Zooms to show the morphologies of the printed structures (top view C, tilted view D).
This example demonstrates the high potential of laser printing process as a high resolution additive microfabrication technology. Reprint with permission from Ref. [120].

between the donor and the receiver substrates. To demonstrate this capability, the same authors have also printed a complex logo inside a 300-µm-wide and 150-µm-deep blind via [121]. The printing distance was 300 µm, and a resolution of the order of 10 µm has been demonstrated. Such a high-resolution and easy-to-implement printing technique for metals is of particular interest for interconnection applications. It allows printing metal lines as thin as few micrometers and with a thickness directly controlled by the number of overlapping pixels [121]. There are unique advantages to using this LIFT technique in this context. First, the molten droplets solidify as soon as they reach the receiver substrate, and second, the process does not require any thermal post-treatment to obtain the conductive properties, as for silver inks. This allows printing lines on any thermally sensitive substrates or filling via with high aspect ratios. A concern remains that the transfer of hot liquid metal in air at atmospheric pressure leads to oxidation of the metal droplets, which can affect the electrical performances of the printed structures. LIFT-printed copper lines exhibit typical resistivities ranging from 4 to 14 times the resistivity of bulk monocrystalline copper [122]. However, the authors do not attribute these high resistivity values to the oxidation process, but on the structural properties of the printed structures, including the formation of nano-grains inducing electron scattering and an amorphous layer at the droplet boundaries. When aluminum structures are printed, the oxidation mechanisms have a significant impact on their electrical properties. However, experiments show that changing the printing conditions allows adjusting the resistivity of the printed material in an exploitable range [123]. Taken together, these demonstrations make LIFT of metal in the liquid phase from a solid donor appears a very attractive technology for the printing of high-resolution interconnects for microelectronic applications.

The transfer of micro-pixels of pure metal or alloys instead of droplets of metal nanoparticle inks opens also a way for digital micro-fabrication in the three dimensions. Indeed, depending on the volume of the ejected material and on the distance between the donor and the receiver substrates, the LIFTed dots can solidify before reaching the receiver. Even if they are not cooled enough to land as solid dots, the heat diffusion in the substrate can be used to dissipate the remaining thermal load, which a very fast solidification process. Then, the printing of successive dots at the same location leads to the formation of high-aspect-ratio pillars. Figure 11 shows a set of laser-printed copper pillars whose length increases with the number of ejected dots [124]. Using this approach, Visser et al. built gold and copper pillars with diameter smaller than 5 µm

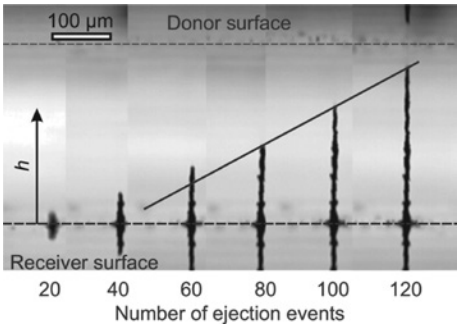


**Figure 11:** Snapshots of a pillar as a function of the number of ejections.
The solid line indicates a constant pillar growth rate of 2.3 µm per ejection. Reprint with permission from Ref. [124].

and lengths up to 2 mm with homogeneous mechanical properties [124]. Recently, this group fabricated more complex structures with true 3D control, as for instance a freestanding thermocouple made of two bended pillars of different materials, gold and platinum, and exhibiting a linear response to the temperature [125]. This result demonstrates the ability of this laser digital printing method to manufacture functional microdevices.

One can observe in the previous figures, and those of related references, that the printing of metal from solid donors with single laser pulses allows the fabrication of 3D microstructures, but it also generates some unwanted droplets around the printed structures. In the double-pulse LIFT technique, this issue is solved because the ultrashort laser triggers the jet formation from a metal liquid film. Then, as for the standard LIFT in the liquid phase [102], this approach leads to the formation of solid single microdroplets without any satellites around. Fabrication of 2D and 3D metal microstructures can still be achieved by printing successive dots next to each other or on the top of each other. Figure 12A shows a pillar made of five successive transfers with double-pulse LIFT from a 1-µm-thick copper film. This pillar exhibits a base with a larger diameter, which corresponds to the first printed dot. Indeed, the first liquid metal jet lands on a glass substrate with a low heat diffusion coefficient compared with copper, and it takes some time to cool down. So, the liquid copper spreads onto the surface before its solidification with quite flat shape (see insert). On the contrary, the following jets arrive on a copper material with a high heat diffusion coefficient and they solidify with an elongated shape. As shown in Figure 9, the shape of the ejected liquid metal can be tuned by increasing the laser fluence from a single droplet to a jet with increasing length. More control can be demonstrated when the transfer occurs through a droplet formation because the volume of the ejected liquid is smaller

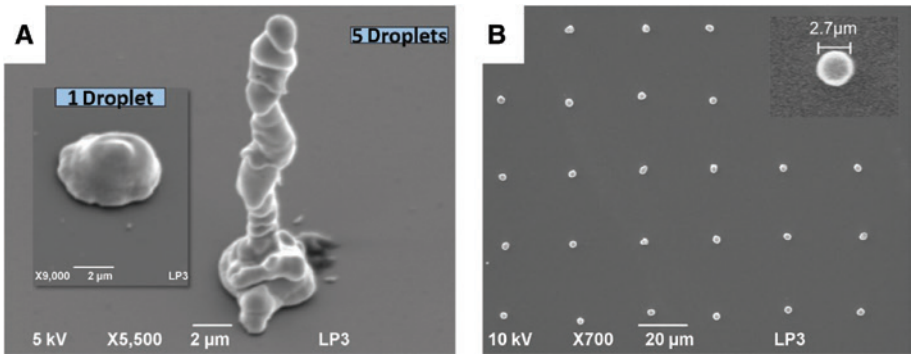


**Figure 12:** 2D copper structures laser printed with double pulse LIFT approach.
Pillar of copper microdroplets (A) and array of copper microdots (B) printed with double-pulse LIFT technique.

than the one in a jet and the cooling is faster. Ultimately, if the gap between the donor and the receiver substrates is large enough, the droplet solidifies during the transfer and reaches the receiver in the solid phase with a spherical shape. Figure 12B shows an array of such copper microdots with a zoom on a single dot with a 2.7 µm diameter.

## 4 Digital laser nanoprinting

Laser printing of nanoparticles has been recently introduced as a branch of LIFT technology for printing of very small and delicate objects [114, 115, 126]. The diameter of the laser-printed droplets depends on the volume of the transferred material. To downscale the size of the printed structures from micro to nano, it is then mandatory to reduce the amount of ejected liquid. To do so, both the film thickness and the laser spot size need to be minimized. Based on this approach, femtosecond laser printing has been applied for the controlled fabrication of metal (Au, Ag, Cu, Fe, etc.) [105–107], alloy ($FeSi_2$) [127], and semiconductor (Si, Ge, etc.) [126, 128] nanoparticles. The transfer mechanisms rely on different melting dynamics that are material dependent and can be accompanied by a broad variety of structural changes. These studies demonstrated the ability of the LIFT process to print nanodots with controllable sizes, spherical shape, and different crystallographic phase [126, 129]. In those experimental works, the thicknesses of the donor films are smaller than 100 nm, the laser spot diameters are smaller than 4 µm, and laser pulses with 100 fs duration or shorter were used. Usually, laser pulses are focused by a long-distance microscope objective, which allows printing nanoparticles both in the forward and backward directions.

The generation of silicon nanoparticles has attracted considerable attention during the recent years because of their pronounced magnetic and electric dipole resonances. These resonances are located in the visible spectrum if the nanoparticle diameter is in the range of 100–200 nm. LIBT has been successively used to print silicon nanoparticles with diameter ranging from 160 to 240 nm [126]. The particle sizes were tuned by varying the laser fluence, and that led to a change in the resonance positions. Figure 13 shows SEM images of LIBT-printed Si particles with different diameters and the corresponding optical response under dark field microscope illumination.

Recently, crystalline Ge and $Si_{1-x}$ $Ge_x$ nanoparticles, with diameters as small as 100 nm, have been laser printed from an amorphous donor film. Beyond the control of the morphological characteristics of these nanoparticles, thanks to the printing conditions (film thickness and laser fluence), the experimental measurements of their resonant optical responses, corresponding to electric and magnetic dipole contributions, are in good agreement with the theoretical calculations based on the Mie theory [128]. LIFT of nanodots has also demonstrated its ability to control the crystalline structures of the deposited materials. Indeed, depending on the volume of the ejected nanoparticle and on the travelling distance between the donor and the receiver, the dynamics of the cooling and solidification processes are different. For pure metals, as previously mentioned, a study points out that the formation of nano-grains inside the printed copper microparticles surrounded by an amorphous layer reduces the conductive properties of fabricated structures [122]. More recently, a specific study was dedicated to the influence of the donor-receiver distance on the structural properties of silicon nanoparticles [130]. Figure 14 shows a schematic illustration of this study. The donor substrate was a 50-nm a-Si:H film and the transfers were induced by irradiations with 50-fs laser pulses (red beams in Figure 14). Printing has been performed for donor-receiver gaps ranging from 5 to 56 µm, and the optical properties of the printed silicon

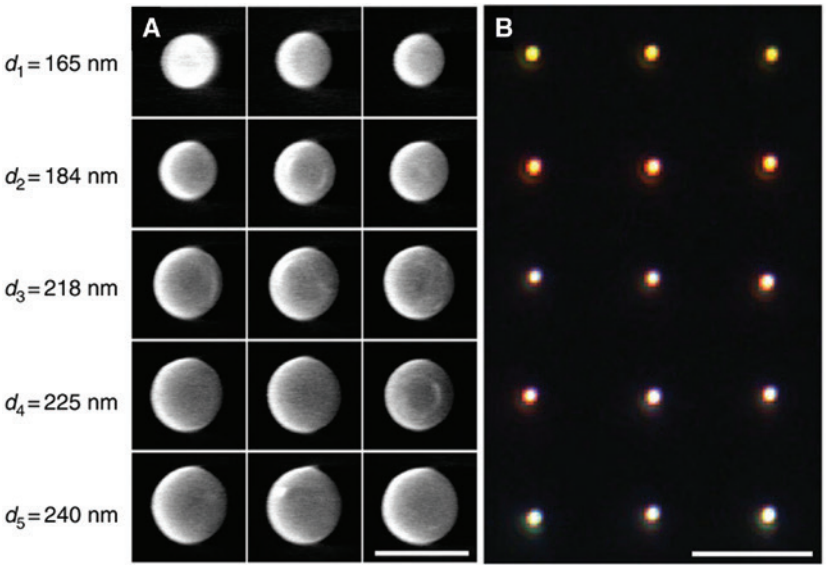


**Figure 13:** Laser pulse energy dependence of the silicon nanoparticle diameter.
(A) SEM images of nanoparticles fabricated at slightly different laser pulse energies starting from 5 nJ. Each line, from top to bottom, corresponds to the laser pulse energy increase of ≈0.1 nJ (scale bar, 300 nm). (B) Changes in the optical response of the generated nanoparticles are visualized by dark-field microscopic images (scale bar, 5 mm). Reprinted with permission from Ref. [126].

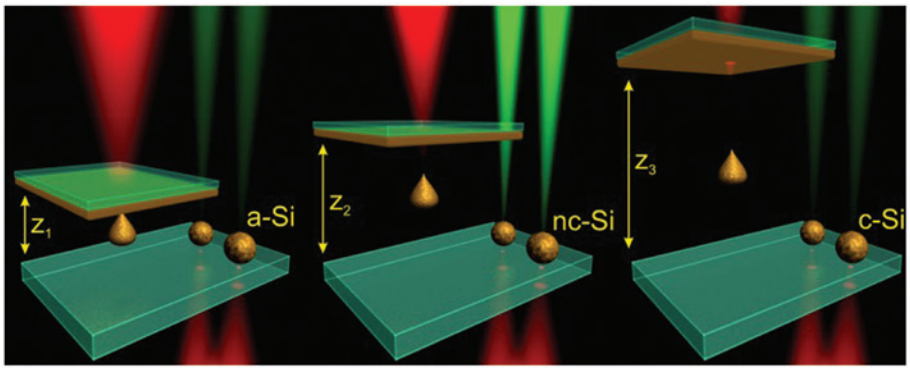


**Figure 14:** Schematic illustration of laser printing of silicon nanoparticles at different distances between donor (upper) and receiver (lower) substrates and the impact on their crystalline structure. The red beam represents the laser printing pulse while the green beams correspond to Raman measurement.
Reprinted with permission from Ref. [130].

droplets were characterized by Raman spectroscopy (green beams in Figure 14). The authors show that for short gap values (<10 μm), the printed Si particles are amorphous, while large gaps (>20 μm) lead to the deposition of crystalline nanoparticles. In between, the structure of the printed droplets exhibits amorphous phase and grain size around 40 nm, which corresponds to the maximum efficiency of second harmonic generation. Numerical simulations confirmed that the crystalline structure of these nanoparticles is controlled by the cooling rate of the material.

Another important benefit of this laser transfer process is its ability to provide an accurate positioning of the nanoparticles on the receiver substrate. For instance, LIBT has been used to print sets of two silicon nanoparticles of 190 nm diameter with separation distance tuned between 375 nm and 5 nm [131]. The authors demonstrated that the resonant optical behavior of these dimers is dependent on the inter-particle distance, and as a consequence, laser printing appears as a versatile and precise technique to fabricate advanced metasurfaces with customized optical properties.

The laser printing technique is not only capable of generating 2D nanoparticle structures. Indeed, by independent movement of the donor and receiver substrates, it is also possible to achieve a targeted stacking of several thousands of nanoparticles. A first demonstration of this

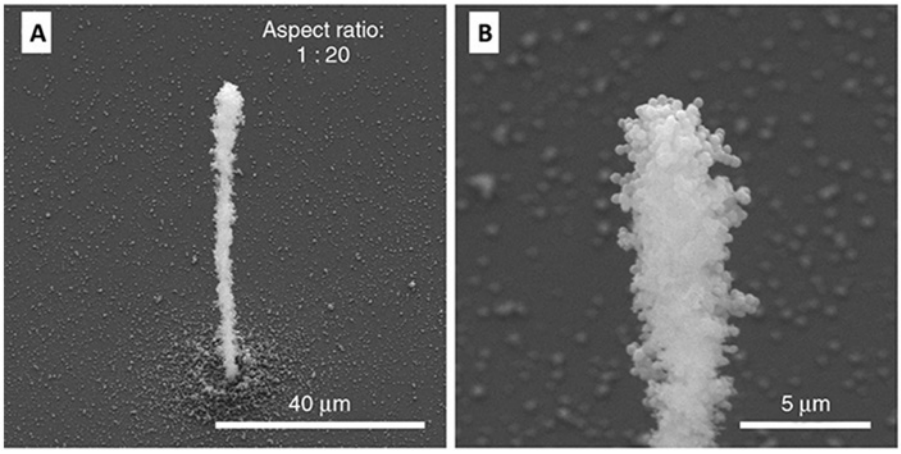


**Figure 15:** Three-dimensional structure consisting of several thousands of silicon nanoparticles generated by laser printing. Pillar of 60 µm high and 3 µm width (A) and the zoom on the top of the pillar shows that it is composed of silicon nanoparticles (B).

approach is shown in Figure 15. The structure that is 60 µm in height and 3 µm in width is made of 10,000 silicon transferred nanoparticles. Each nanoparticle within the structure has a diameter of about 250 nm. This proof-of-principle demonstration directly shows the capabilities of the laser printing process and its applicability as a new method for high-resolution additive manufacturing of 3D structures with sub-µm resolution.

## 5 Laser printing of nanophotonic devices

In the perspective of using laser printing for the fabrication of nanophotonics devices, we have pointed out some of the unique features of this technology, which are the control of the printed particle sizes down to 100 nm, the high resolution of the positioning, the wide range of printable materials, and the ability to print nano-objects with various crystalline structures. Based on these capabilities, some nanophotonics devices have already been fabricated and tested. For instance, a plasmonic biosensor has been realized, and its performances, quantified [132]. For this purpose, the sizes of the laser-printed nanoparticles have been reduced by using lithographically structured films consisting of small islands of material [132–135]. After laser irradiation to transfer the structures, the material islands contract into spherical nanoparticles due to surface tension. The sizes of the nanoparticles in this case can be much smaller, in the range of a few tens of nanometers, and are precisely determined by the volume of the material islands [133]. The authors showed that such laser-fabricated metasurfaces provide resonances with nearly zero intensity in reflected light for p-polarized light, yielding to the generation of phase singularities. Such an optical sensor exhibits a sensitivity of $5\times10^4$ deg./RIU (refractive index unit) and a limit of detection lower than $10^7$ RIU, which is comparable to or better than the performances of commercial amplitude-sensitive surface plasmon resonance systems [132]. It is worth mentioning a recent study dedicated to the laser printing of a new kind of nanoantennas. Tiguntseva et al. have printed halide perovskite nanoparticles to create light-emitting nanoantennas, which exhibit strong photoluminescence in the range of 530 – 770 nm depending on their composition [136]. Local nano-heating by the irradiation of metal nanoparticles is a mechanism that has already exploited for nano-imaging [6, 137]. LIFT has been used to print silicon nanoparticles that have the ability to convert light to heat with up to 4 times more efficiency than similar spherical gold nanoparticles [138]. The advantage of using crystalline silicon is the simplicity of local temperature control by means of Raman spectroscopy working in a broad range of temperatures, that is, up to the melting point of silicon (1690 K) with sub-micrometer spatial resolution.

Tseng et al. have used another unique advantage of the laser printing technique to transfer split-ring resonator (SRR) structures in order to fabricate plasmonic metamaterials [139]. Indeed, LIFT allows printing multilayer materials in a single step when these layers are previously deposited on the donor substrates [88]. Figure 16 is a schematic description of the process. The printed SRR array exhibits reflection spectra in very good agreement with finite-difference time-domain simulations and excellent resonant properties.

Beyond these first demonstrations and the realization of nanoantennas and plasmonics-based sensors,

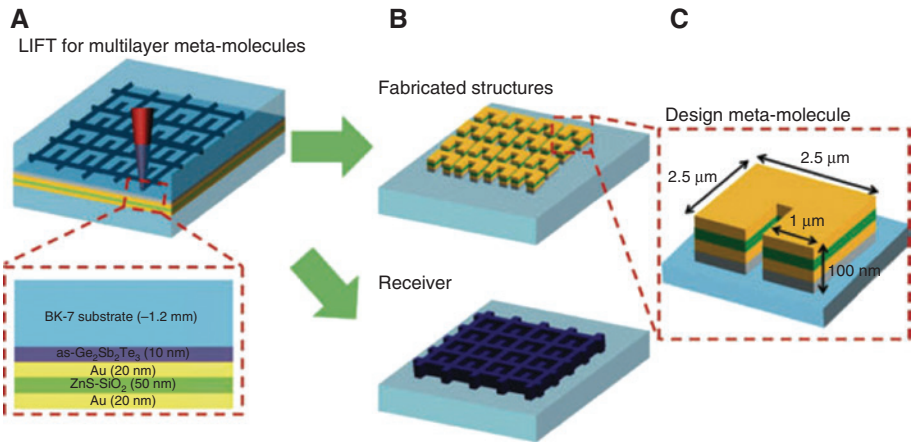


**Figure 16:** Fabrication of multilayer metamaterials by femtosecond laser-induced forward-transfer technique.
(A) Schematics of the fabrication method of the multilayer structures by contact-mode LIFT technique. (B) Separating the laser-processed donor-receiver pair, the fabricated multilayer metamaterials can be obtained. (C) Feature size of design multilayer metamaterial. Reprinted with permission from Ref. [139].

laser printing appears as a very attractive method to easily fabricate a wide set of new nanophotonics devices. For instance, hybrid Si/Au nanoparticles have been recently used to generate white light at the nanoscale, thanks to their efficient photoluminescence characteristics [140]. This offers the possibility to measure the near-field response in a broad spectral range and to realize ultra-broadband near-field nanospectroscopy. Laser printing is a very powerful method used to print hybrid nanoparticles from multilayer films [127, 141] with tunable properties by changing the donor film characteristics. Thus, it is a very relevant approach to fabricate nanospectroscopy devices.

## 6 Conclusion

Laser printing has demonstrated its ability to transfer small volumes of liquids, from picoliters to attoliters, on a substrate to form particles with corresponding diameters ranging from 100 nm to a few micrometers. These micro- and nanoparticles have been printed from various materials and even arranged in 3D structures. Moreover, this process can be performed in air without any protective gas atmosphere, which is an important technological advantage. As the required laser energy for ejecting such small amount of matter is very low, the use of femtosecond oscillator operating in the MHz range can be considered for this application. This, combined with fast beam motion technologies, has the potential to open the way to high printing throughputs.

Surely, there are still some important challenges to face, including the positioning resolution and the limitation of undesired debris, before the LIFT process becomes a reliable nanoprinting technology. However, one finds already in LIFT an unprecedented level of flexibility that attracts considerable interest. This will undoubtedly lead to further advances in the near future. For instance, extra-optimization on the mechanical properties of the donor film is expected by adjusting its composition by adding a small amount of dopants or working with multilayer films [141]. One may also expect the emergence of other pre-pulse strategies to locally modify the material properties under melting of the donor film. Temporal and spatial beam shaping [142, 143] is also aspect to be considered to optimize the energy deposition, the fluid motion and the generation of localized high pressure. Looking at the potential applications, laser printing can become a highly flexible, and digital, method for 3D high-resolution additive manufacturing and holds the potential to drastically change how optical and electronic micro- and nanodevices are designed and fabricated today.

**Acknowledgment:** The project leading to this publication has received funding from the Excellence Initiative of Aix-Marseille University – A*Midex, a French “Investissements d’Avenir” program.

## References

[1] Zorba V, Stratakis E, Barberoglou M, et al. Biomimetic artificial surfaces quantitatively reproduce the water repellency of a lotus leaf. Adv Mater 2008;20:4049.
[2] Feng L, Zhang Y, Xi J, et al. Petal effect: a superhydrophobic state with high adhesive force. Langmuir 2008;24:4114–9.

[3] Hermens U, Kirner SV, Emonts C, et al. Mimicking lizard-like surface structures upon ultrashort laser pulse irradiation of inorganic materials. Appl Surf Sci 217;418:499–507.
[4] Yu N, Capasso F. Flat optics with designer metasurfaces. Nat Mater 2014;13:139–50.
[5] Proust J, Bedu F, Gallas B, Ozerov I, Bonod N. All-dielectric colored metasurfaces with silicon Mie resonators. ACS Nano 2016;10:7761–7.
[6] Baffou G, Quidant R. Thermo-plasmonics: using metallic nanostructures as nano-sources of heat. Laser Photonics Rev 2013;7:171–87.
[7] Mo YF, Turner KT, Szlufarska I. Friction laws at the nanoscale. Nature 2009;457:1116–9.
[8] Rao YQ, Pochan JM. Mechanics of polymer-clay nanocomposites. Macromolecules 2007;40:290–6.
[9] Lal S, Link S, Halas NJ. Nano-optics from sensing to waveguiding. Nat Photon 2007;1:641–8.
[10] Kabashin AV, Evans P, Pastkovsky S. Plasmonic nanorod metamaterials for biosensing. Nat Mater 2009;8:867–71.
[11] Barth JV. Molecular architectonic on metal surfaces. Ann Rev Phys Chem 2007;58:375–407.
[12] Baffou G, Quidant R. Nanoplasmonics for chemistry. Chem Soc Rev 2014;43:3898–907.
[13] Chen GY, Qju HL, Prasad PN, Chen XY. Upconversion Nanoparticles: design, nanochemistry, and applications in theranostics. Chem Rev 2014;114:5161–214.
[14] Brongersma ML, Cui Y, Fan Sh. Light management for photovoltaics using high-index nanostructures. Nat Mater 2014;13:451–60.
[15] Gao H, Liu C, Jeong HE, Yang P. Plasmon-enhanced photocatalytic activity of iron oxide on gold nanopillars. ACS Nano 2012;6:234–40.
[16] Maksymov IS, Staude I, Miroshnichenko AE, Kivshar YS. Optical Yagi-Uda nanoantennas. Nanophotonics 2012;1:65–81.
[17] Ho J, Fu YH, Dong Z, et al. Highly directive hybrid metal-dielectric Yagi-Uda nanoantennas. ACS Nano 2018;12:8616–24.
[18] Deng JH, Fu J, Ng J, Huang ZF. Tailorable chiroptical activity of metallic nanospiral arrays. Nanoscale 2016;8:4504–10.
[19] Stout B, Devilez A, Rolly B, Bonod N. Multipole methods for nano-antennas design: applications to Yagi-Uda configurations. J Opt Soc Am B 2011;28:1213–23.
[20] Ni X, Emani NK, Kildishev AV, Boltasseva A, Shalaev VM. Broadband light bending with plasmonic nanoantennas. Science 2012;335:427.
[21] Guo L. Nanoimprint lithography: methods and material requirements. Advanced Materials 2007;19:495–513.
[22] Bottein T, Dalstein O, Putero M, et al. Environment-controlled sol-gel soft-NIL processing for optimized titania, alumina, silica and yttria-zirconia imprinting at sub-micron dimensions. Nanoscale 2018;10:1420–31.
[23] Ruiz SA, Chen CS. Microcontact printing: a tool to pattern. Soft Matter 2007;3:168–77.
[24] Loo YL, Willett RL, Baldwin KW, Rogers JA. Interfacial chemistries for nanoscale transfer printing. J Am Chem Soc 2002;124:7654–5.
[25] Wang H, Wen L, Hu X, Yu Y, Zhao Y, Chen Q. Nanoscale printing technique and its applications in nanophotonics. Nano 2016;11:1630002.
[26] Kabashin AV, Delaporte Ph, Pereira A, et al. Nanofabrication with pulsed lasers. Nanoscale Res Lett 2010;5:454–63.
[27] Grojo D, Boarino L, De Leo N, et al. Size scaling of mesoporous silica membranes produced by nanosphere mediated laser ablation. Nanotechnology 2012;23:485305.
[28] Pereira A, Grojo D, Chaker M, Delaporte Ph, Guay D, Sentis M. Laser-fabricated porous alumina membrane (LF-PAM) for the preparation of metal nanodot arrays. Small 2008;4:572–5.
[29] Lasagni A, D'Alessandria M, Giovanelli R, Mucklich F. Advanced design of periodical architectures in bulk metals by means of laser interference metallurgy. Appl Surf Sci 2007;254:930–6.
[30] Rank A, Lang V, Lasagni AF. High-speed roll-to-roll hot embossing of micrometer and sub micrometer structures using seamless direct laser interference patterning treated sleeves. Adv Eng Mat 2017;19:1700201.
[31] Vorobyev AY, Guo CL. Direct femtosecond laser surface nano/microstructuring and its applications. Laser Photonics Rev 2013;7:385–407.
[32] Tull BR, Carey JE, Mazur E, McDonald JP, Yalisove SM. Silicon surface morphologies after femtosecond laser irradiation. MRS Bull 2006;31:626–33.
[33] Halbwax M, Sarnet T, Hermann J, et al. Micromachining of semiconductor by femtosecond laser for integrated circuit defect analysis. Appl Surf Sci 2007;254:911–5.
[34] Halbwax M, Sarnet T, Delaporte Ph, et al. Micro and nano-structuration of silicon by femtosecond laser: application to silicon photovoltaic cells fabrication. Thin Solid Films 2008;516:6791–5.
[35] Carey JE, Crouch CH, Shen MY, Mazur E. Visible and near-infrared responsivity of femtosecond-laser microstructured silicon photodiodes. Opt Lett 2005;30:1773–5.
[36] Kirner SV, Hermens U, Mimidis A, et al. Mimicking bug-like surface structures and their fluid transport produced by ultrashort laser pulse irradiation of steel. Appl Phys A 2017;123:754.
[37] Dusser B, Sagan Z, Soder H, et al. Controlled nanostructrures formation by ultra fast laser pulses for color marking. Opt Express 2010;18;2913–24.
[38] Henley SJ, Carey JD, Silva SRP. Pulsed-laser-induced nanoscale island formation in thin metal-on-oxide films. Phys Rev B 2005;72:195408.
[39] Tseng ML, Chang CM, Cheng BH, et al. Multi-level surface enhanced Raman scattering using $AgO_x$ thin film. Opt Express 2013;21:24460.
[40] Chen HM, Chen CK, Tseng ML. Plasmonic ZnO/Ag embedded structures as collecting layers for photogenerating electrons in solar hydrogen generation photoelectrodes. Small 2013;9:2926.
[41] Tseng ML, Huang YW, Hsiao MK, et al. Fast fabrication of a Ag nanostructure substrate using the femtosecond laser for broad-band and tunable plasmonic enhancement. ACS Nano 2012;6:5190.
[42] Nakata Y, Miyanaga N, Okada T. Effect of pulse width and fluence of femtosecond laser on the size of nanobump array. Appl Surf Sci 2007;253:6555–7.
[43] Moening JP, Thanawala SS, Georgiev DG. Formation of high aspect-ratio protrusions on gold films by localized pulsed laser irradiation. Appl Phys A 2009;95:635–8.
[44] Chang CM, Chu CH. Light manipulation by gold nanobumps. Plasmonics 2012;7:563–9.
[45] Nakata Y, Miyanaga N, Momoo K, Hiromoto T. Solid-liquid-solid process for forming free-standing gold nanowhisker superlattice by interfering femtosecond laser irradiation. Appl Surf Sci 2013;274:27–32.

[46] Chang CM, Tseng ML, Cheng BH, et al. Three-dimensional plasmonic micro projector for light manipulation. Adv Mater 2013;25:1118–23.
[47] Singh M, Haverinen HM, Dhagat P, Jabbour GE. Inkjet printing-process and its applications. Adv Mater 2010;22:673–85.
[48] Torrisi F, Hasan T, Wu WP, et al. Inkjet-printed graphene electronics. ACS Nano 2012;6:2992–3006.
[49] Galliker P, Schneider J, Eghlidi H, Kress S, Sandoghdar V, Poulikakos D. Direct printing of nanostructures by electrostatic autofocussing of ink nanodroplets. Nat Com 2012;3:890.
[50] Galliker P, Schneider J, Poulikakos D. Dielectrophoretic bending of directly printed free-standing ultra-soft nanowires. Appl Phys Lett 2014;104:073105.
[51] Farsari M, Chichkov BN. Two-photon fabrication. Nat Photon 2009;3:450–2.
[52] Kawata S, Sun H-B, Tanaka T, Takada K. Finer features for functional microdevices. Nature 2001;412:697–8.
[53] Aristov AI, Manousidaki M, Danilov A et al. 3D plasmonic crystal metamaterials for ultra-sensitive biosensing. Sci Rep 2016;6:25380.
[54] Doraiswamy A, Jin C, Narayan RJ, et al. Two photon induced polymerization of organic-inorganic hybrid biomaterials for microstructured medical devices. Acta Biomater 2006;2:267–75.
[55] Melissinaki V, Gill AA, Ortega I, et al. Direct laser writing of 3D scaffolds for neural tissue engineering. Biofabrication 2011;3:045005.
[56] Waller EH, Von Freymann G. From photoinduced electron transfer to 3D metal microstructures via direct laser writing. Nanophotonics 2018;7:1259–77.
[57] Kuznetsov AI, Unger C, Koch J, Chichkov BN. Laser-induced jet formation and droplet ejection from thin metal films. Appl Phys A 2012;106:479–87.
[58] Bohandy J, Kim BF, Adrian FJ. Metal deposition from a supported metal film using an excimer laser. J Appl Phys 1986;60:1538–9.
[59] Auyeung RCY, Kim H, Birnbaum AJ, Zalalutdinov M, Mathews SA, Piqué A. Laser decal transfer of freestanding microcantilevers and microbridges. Appl Phys A 2009;97:513–9.
[60] Kattamis NT, McDaniel ND, Bernhard S, Arnold CB. Laser direct write printing of sensitive and robust light emitting organic molecules. Appl Phys Lett 2009;94:103306.
[61] Duocastella M, Patrascioiu A, Fernández-Pradas JM, Morenza JL, Serra P. Film-free laser forward printing of transparent and weakly absorbing liquids. Opt Express 2010;18:21815–25.
[62] Li Q, Alloncle AP, Grojo D, Delaporte Ph. Generating liquid nanojets from copper by dual laser irradiation for ultra-high resolution printing. Opt Express 2017;25:24164–72.
[63] Di Pietrantonio F, Benetti M, Cannatà D, et al. Volatile toxic compound detection by surface acoustic wave sensor array coated with chemoselective polymers deposited by laser induced forward transfer: application to sarin. Sens Actuators B 2012;174:158–67.
[64] Touloupakis E, Boutopoulos C, Buonasera K, Zergioti I, Giardi MT. A photosynthetic biosensor with enhanced electron transfer generation realized by laser printing technology. Anal Bioanal Chem 2012;402:3237–44.
[65] Fardel R, Nagel M, Nüesch F, Lippert T, Wokaun A. Fabrication of organic light-emitting diode pixels by laser-assisted forward transfer. Appl Phys Lett 2007;91:061103.
[66] Kattamis NT, McDaniel NT, Bernhard S, Arnold CB. Ambient laser direct-write printing of a patterned organo-metallic electroluminescent device. Organ Electron 2011;12:1152–8.
[67] Rapp L, Diallo AK, Alloncle AP, Videlot-Ackerman C, Fages F, Delaporte Ph. Pulsed-laser printing of organic thin film transistors. Appl Phys Lett 2009;95:171109.
[68] Rapp L, Biver E, Alloncle AP, Delaporte Ph. High-speed laser printing of silver nanoparticles ink. J Laser Micro/Nanoeng 2014;9:5–9.
[69] Hennig G, Baldermann Th, Nussbaum Ch, et al. Lasersonic LIFT process for large area digital printing. J Laser Micro/Nanoeng 2012;7:299–305.
[70] Serra P, Colina M, Fernández-Pradas JM, Sevilla L, Morenza JL. Preparation of functional DNA microarrays through laser-induced forward transfer. Appl Phys Lett 2004;85:1639.
[71] Zergioti I, Karaiskou A, Papazoglou DG, Fotakis C, Kapsetaki M, Kafetzopoulos D. Femtosecond laser microprinting of biomaterials. Appl Phys Lett 2005;86:163902.
[72] Doraiswamy A, Narayan R, Lippert T, et al. Excimer laser forward transfer of mammalian cells using a novel triazene absorbing layer. Appl Surf Sci 2006;249:4743–7.
[73] Guillotin B, Souquet A, Catros S, et al. Laser assisted bioprinting of engineered tissue with high cell density and microscale organization. Biomaterials 2010;31:7250–6.
[74] Gruene M, Pflaum M, Hess C, et al. Laser printing of three-dimensional multicellular arrays for studies of cell-cell and cell-environment interactions. Tissue Eng Part C 2011;17:973–82.
[75] Kim H, Charipar NA, Birnbaum AJ, Mathews SA, Piqué A. Laser forward transfer based on a spatial light modulator. Appl Phys A 2011;102:21–6.
[76] Wang J, Auyeung RCY, Kim H, Charipar NA, Piqué A. Three-dimensional printing of interconnects by laser direct-write of silver nanopastes. Adv Mater 2010;22:4462–6.
[77] Su V, Chu CH, Sun G, Tsai DP. Advances in optical metasurfaces: fabrication and applications [invited]. Opt Express 2018;26:13148.
[78] Delaporte Ph, Alloncle AP. Laser-induced forward transfer: a high resolution additive manufacturing technology [invited paper]. J Opt Laser Technol 2016;78:33–41.
[79] Duocastella M, Fernández-Pradas JM, Morenza JL, Serra P. Time-resolved imaging of the laser forward transfer of liquids. J Appl Phys 2009;106:084907.
[80] Piqué E, Serra P. Laser printing of functional materials: 3D microfabrication, Electronics and Biomedicine. Weinheim, Wiley-VCH, 2018.
[81] Duocastella M, Heungsoo K, Serra P, Piqué A. Optimization of laser printing of nanoparticle suspensions for microelectronic applications [invited paper]. Appl Phys A 2012;106:471–8.
[82] Nagel M, Lippert T. Laser-induced forward transfer for the fabrication of devices. In: Singh SC, Zeng H, Guo C, Cai W, eds., Nanomaterials: processing and characterization with lasers. Weinheim, Wiley-VCH, 2012, 255–316.
[83] Feinaeugle M, Alloncle AP, Delaporte Ph, Sones CL, Eason RW. Time-resolved shadowgraph imaging of femtosecond laser-induced forward transfer of solid materials. Appl Surf Sci 2012;258:8475–83.
[84] Fardel R, Nagel M, Nuesch F, Lippert T, Wokaun A. Laser-induced forward transfer of organic LED building blocks studied by time-resolved shadowgraphy. J Phys Chem C 2010;114:5617–36.
[85] Nagel M, Hany R, Lippert T, Molberg M, Nüesch FA, Rentsch D. Aryltriazene photopolymers for UV-laser applications: improved synthesis and photodecomposition study. Macromol Chem Phys 2007;208:277–86.

[86] Rapp L, Diallo AK, Nénon S, et al. Laser printing of a semiconducting oligomer as active layer in organic thin film transistors: impact of a protecting triazene layer. Thin Solid Films 2012;520:3043–7.
[87] Rapp L, Constantinescu C, Larmande Y, Alloncle AP, Delaporte P. Smart beam shaping for the deposition of solid polymeric material by laser forward transfer. Appl Phys A 2014;117:333–9.
[88] Shaw-Stewart J, Lippert T, Nagel M, Nüesch F, Wokaun A. Red-green-blue polymer light-emitting diode pixels printed by optimized laser-induced forward transfer. Appl Phys Lett 2012;100:203303.
[89] Rapp L, Constantinescu C, Larmande Y, et al. Functional multilayered capacitor pixels printed by picosecond laser-induced forward transfer using a smart beam shaping technique. Sens Actuators A 2015;224:111–8.
[90] Rapp L, Constantinescu C, Delaporte Ph, Alloncle AP. Laser-induced forward transfer of polythiophene-based derivatives for fully polymeric thin film transistors. Organ Electron 2014;15:1868–75.
[91] Pearson A, Cox E, Blake JR, Otto SR. Bubble interactions near a free surface. Eng Anal Bound Elem 2004;28:295–313.
[92] Duocastella M, Fernández-Pradas JM, Serra P, Morenza JL. Sessile droplet formation in the laser-induced forward transfer of liquids: a time-resolved imaging study. Thin Solid Films 2010;518:5321–5.
[93] Biver E, Rapp L, Alloncle AP, Serra P, Delaporte Ph. High-speed multi-jets printing using laser forward transfer: time-resolved study of the ejection dynamics. Opt Express 2014;22:17122–34.
[94] Boutopoulos Ch, Kalpyris I, Serpetzoglou E, Zergioti I. Laser-induced forward transfer of silver nanoparticle ink: time-resolved imaging of the jetting dynamics and correlation with the printing quality. Microfluid Nanofluid 2014;16:493–500.
[95] Koch L, Deiwick A, Schlie S. Skin tissue generation by laser cell printing. Biotechnol Bioeng 2012;109:1855–63.
[96] Fernandez-Pradas JM, Colina M, Serra P, Domınguez J, Morenza JL. Laser-induced forward transfer of biomolecules. Thin Solid Films 2004;453–454:27–30.
[97] Zergioti I, Karaiskou A, Papazoglou DG, Fotakis C, Kapsetaki M, Kafetzopoulos D. Time resolved Schlieren study of sub-picosecond and nanosecond laser transfer of biomaterials. Appl Surf Sci 2005;247:584–9.
[98] Guillemot F, Souquet A, Catros S, et al. High-throughput laser printing of cells and biomaterials for tissue engineering. Acta Biomater 2010;6:2494–500.
[99] Ringeisen BR, Kim H, Barron JA. Laser printing of pluripotent embryonal carcinoma cells. Tissue Eng 2004;10:483–91.
[100] Florian C, Caballero-Lucas F, Fernández-Pradas JM, et al. Conductive silver ink printing through the laser-induced forward transfer technique. Appl Surf Sci 2015;336:304–8.
[101] Makrygianni M, Kalpyris I, Boutopoulos C, Zergioti I. Laser induced forward transfer of Ag nanoparticles ink deposition and characterization. Appl Surf Sci 2014;297:40–4.
[102] Rapp L, Ailuno J, Alloncle AP, Delaporte Ph. Pulsed-laser printing of silver nanoparticles ink: control of morphological properties. Opt Express 2011;19:21563–74.
[103] Puerto D, Biver E, Alloncle AP, Delaporte Ph. Single step high-speed printing of continuous silver lines by laser-induced forward transfer. Appl Surf Sci 2016;374:183–9.
[104] Turkoz E, Perazzo A, Kim H, Stone HA, Arnold CB. Impulsively induced jets from viscoelastic films for high-resolution printing. Phys Rev Lett 2018;120:074501.
[105] Banks DP, Grivas C, Mills JD, Eason RW, Zergioti I. Nanodroplets deposited in micro-arrays by femtosecond Ti:sapphire laser-induced forward transfer. Appl Phys Lett 2006;89:87–90.
[106] Kuznetsov AI, Koch J, Chichkov BN. Laser-induced backward transfer of gold nanodroplets. Opt Express 2009;17:18820–5.
[107] Sametoglu V, Sauer V, Tsui YY. Production of 70-nm Cr dots by laser-induced forward transfer. Opt Express 2013;21:18525–31.
[108] Zenou M, Sa'ar A, Kotler Z. Laser jetting of femto-liter metal droplets for high resolution 3D printed structures. Sci Rep 2015;5:17265.
[109] Pohl R, Visser CW, Römer GW, Lohse D, Sun C, Huis in 't Veld B. Ejection regimes in picosecond laser-induced forward transfer of metals. Phys Rev Appl 2015;3:024001.
[110] Zenou M, Sa'ar A, Kotler Z. Supersonic laser-induced jetting of aluminum micro-droplets. Appl Phys Lett 2015;106:181905.
[111] Brown MS, Brasz F, Ventikos Y, Arnold CB. Impulsively actuated jets from thin liquid films for high-resolution printing applications. J Fluid Mech 2012;709:341–70.
[112] Ivanov DS, Kuznetsov AI, Lipp VP, et al. Short laser pulse nanostructuring of metals: direct comparison of molecular dynamics modeling and experiment. Appl Phys A 2013;111:675–87.
[113] Shugaev M, Bulgakova N. Thermodynamic and stress analysis of laser-induced forward transfer of metals. Appl Phys A 2010;101:103–9.
[114] Kuznetsov A, Evlyukhin A, Reinhardt C, et al. Laser-induced transfer of metallic nanodroplets for plasmonics and metamaterial applications. J Opt Soc Am B 2009;26:B130–8.
[115] Kuznetsov A, Kiyan R, Chichkov B. Laser fabrication of 2D and 3D metal nanoparticle structures and arrays. Opt Express 2010;18:21198–203.
[116] Anisimov S, Zhakhovsky V, Inogamov N, Murzov S, Khokhlov V. Formation and crystallisation of a liquid jet in a film exposed to a tightly focused laser beam. Quantum Electron 2017;47:509–21.
[117] Unger C, Koch J, Overmeyer L, Chichkov B. Time-resolved studies of femtosecond-laser induced melt dynamics. Opt Express 2012;20:24864–72.
[118] Wu C, Zhigilei LV. Microscopic mechanisms of laser spallation and ablation of metal targets from large-scale molecular dynamics simulations. Appl Phys A 2014;114:11–32.
[119] Inogamov NA, Zhakhovskii VV, Khokhlov VA. Jet formation in spallation of metal film from substrate under action of femtosecond laser pulse. J Exp Theor Phys. 2015;120:15–48.
[120] Zenou M, Sa'ar A, Kotler Z. Laser transfer of metals and metal alloys for digital microfabrication of 3D objects. Small 2015;11:4082–9.
[121] Zenou M, Kotler Z. Printing of metallic 3D micro-objects by laser induced forward transfer. Opt Express 2016;24:1431–46.
[122] Winter S, Zenou M, Kotler Z. Conductivity of laser printed copper structures limited by nano-crystal grain size and amorphous metal droplet shell. J Phys D Appl Phys 2016;49:165310.
[123] Zenou M, Sa'ar A, Kotler Z. Digital laser printing of metal/metal-oxide nano-composites with tunable electrical properties. Nanotechnology 2016;27:015203.

[124] Visser CW, Pohl R, Sun C, Römer GW, Huis in 't Veld B, Lohse D. Toward 3D printing of pure metals by laser-induced forward transfer. Adv Mater 2015;27:4087–92.
[125] Luo J, Pohl R, Qi L, et al. Printing functional 3D microdevices by laser-induced forward transfer. Small 2017;13:1602553.
[126] Zywietz U, Evlyukhin AB, Reinhardt C, Chichkov BN. Laser printing of silicon nanoparticles with resonant optical electric and magnetic responses. Nat Commun 2014;5:3402.
[127] Narazaki A, Sato T, Kurosaki R, Kawaguchi Y, Niino H. Nano- and microdot array formation of $FeSi_2$ by nanosecond excimer laser-induced forward transfer. Appl Phys Express 2008;1:057001.
[128] Zhigunov D, Evlyukhin AB, Shalin AS, Zywietz U, Chichkov BN. Femtosecond laser printing of single Ge and SiGe nanoparticles with electric and magnetic optical resonances. ACS Photon 2018;5:977–83.
[129] Makarov SV, Petrov MI, Zywietz U, et al. Efficient second-harmonic generation in nanocrystalline silicon nanoparticles. Nano Lett 2017;17:3047–53.
[130] Makarov S, Kolotova L, Starikov S, Zywietz U, Chichkov B. Resonant silicon nanoparticles with controllable crystalline state and nonlinear optical response. Nanoscale 2018;10:11403–9.
[131] Zywietz U, Schmidt M, Evlyukhin A, Reinhardt C, Aizpurua J, Chichkov B. Electromagnetic resonances of silicon nanoparticle dimers in the visible. ACS Photon 2015;2:913–20.
[132] Aristov AI, Zywietz U, Evlyukhin AB, Reinhardt C, Chichkov BN, Kabashin AV. Laser-ablative engineering of phase singularities in plasmonic metamaterial arrays for biosensing applications. Appl Phys Lett 2014;104:071101.
[133] Kuznetsov AI, Evlyukhin AB, Goncalves MR, et al. Laser fabrication of large-scale nanoparticle arrays for sensing applications. ACS Nano 2011;5:4843–9.
[134] Sametoglu V, Sauer V, Tsui YY. Nanoscale laser-induced forward transfer through patterned Cr films. Appl Phys A 2013;110:823–7.
[135] Constantinescu C, Deepak KLN, Delaporte Ph, Utéza O, Grojo D. Arrays of metallic micro-/nano-structures by means of colloidal lithography and laser dewetting. Appl Surf Sci 2016;374:124–31.
[136] Tiguntseva EY, Zograf GP, Komissarenko FE, et al. Light-emitting halide Perovskite nanoantennas. Nano Lett 2018:18:1185–90.
[137] Baffou G, Polleux J, Rigneault H, Monneret S. Super-heating and micro-bubble generation around plasmonic nanoparticles under CW illumination. J Phys Chem C 2014;118:4890–8.
[138] Zograf GP, Petrov MI, Zuev DA, et al. Resonant nonplasmonic nanoparticles for efficient temperature-feedback optical heating. Nano Lett 2017;17:2945–52.
[139] Tseng ML, Wu PC, Sun S, et al. Fabrication of multilayer metamaterials by femtosecond laser-induced forward-transfer technique. Laser Photon Rev 2012;6:702–8.
[140] Makarov SV, Sinev IS, Milichko VA, et al. Nanoscale generation of white light for ultrabroadband nanospectroscopy. Nano Lett 2017;8:535–9.
[141] Li Q, Alloncle AP, Grojo D, Delaporte Ph. Laser-induced nano-jetting behaviors of liquid metals. Appl Phys A 2017;123:718.
[142] Stoian R, Boyle M, Thoss A, Rosenfeld A, Korn G, Hertel IV. Dynamic temporal pulse shaping in advanced ultrafast laser material processing. Appl Phys A 2003;77:265–9.
[143] Duocastella M, Arnold CB. Bessel and annular beams for materials processing. Laser Photonics Rev 2012;6:607–21.